

Ab initio calculation of deformed nuclei and the nuclear matrix elements of neutrinoless double beta decay with multi-reference in-medium similarity renormalization group

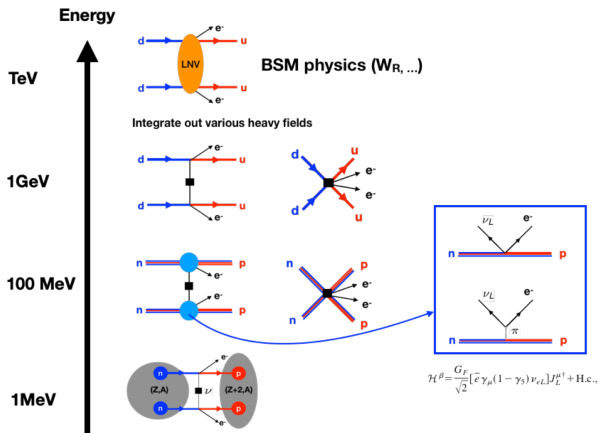
Jiangming Yao

FRIB/NSCL, Michigan State University, East Lansing, Michigan
48824, USA



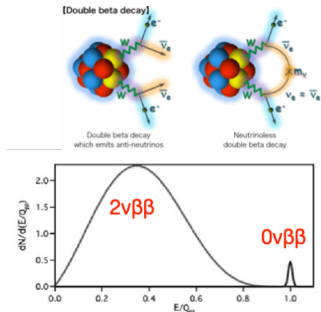
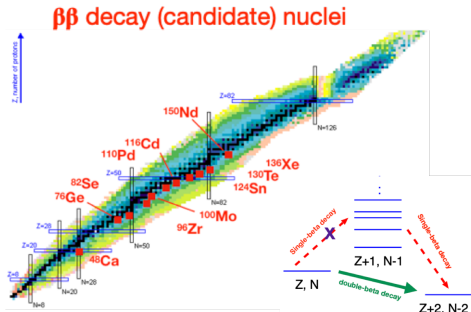
Nuclear seminar at PKU, Beijing, Aug 15, 2019

What's neutrinoless double beta decay? Why interesting?



- Beyond standard model physics: nonzero neutrino mass
- Nature of neutrinos: Dirac or Majorana
- Mechanism for the matter-antimatter asymmetry: LNV

What kind of nuclei to observe the $0\nu\beta\beta$?



The inverse of half-life can be factorized as

$$[T_{1/2}^{0\nu}]^{-1} = g_A^4 G_{0\nu} \left| \frac{\langle m_{\beta\beta} \rangle}{m_e} \right|^2 \left| M^{0\nu}(0_I^+ \rightarrow 0_F^+) \right|^2$$

- phase-space factor $G_{0\nu}$ ($\sim 10^{-14} \text{ yr}^{-1}$)
- effective neutrino mass related to the masses m_k and PMNS mixing matrix U_{ek}

$$\langle m_{\beta\beta} \rangle = \sum_k U_{ek}^2 m_k$$

The 2015 LONG RANGE PLAN for NUCLEAR SCIENCE

RECOMMENDATION II

The excess of matter over antimatter in the universe is one of the most compelling mysteries in all of science. The observation of neutrinoless double beta decay in nuclei would immediately demonstrate that neutrinos are their own antiparticles and would have profound implications for our understanding of the matter-antimatter mystery.

We recommend the timely development and deployment of a U.S.-led ton-scale neutrinoless double beta decay experiment.

A ton-scale instrument designed to search for this as-yet unseen nuclear decay will provide the most powerful test of the particle-antiparticle nature of neutrinos ever performed. With recent experimental breakthroughs pioneered by U.S. physicists and the availability of deep underground laboratories, we are poised to make a major discovery.

【关注】原子能院牵头开展中科院无中微子双贝塔衰变实验咨询项目研究

作者：中国原子能科学研究院 / 公众号：ciayzny 发布时间：2018-09-05

8月25~26日，原子能院组织开展“无中微子双贝塔衰变实验”咨询项目首次研讨会。该咨询项目由张焕乔院士向中科院数理学部成功申请，项目将围绕国内无中微子双贝塔衰变实验的4种方案进行研讨和评估，通过对最先研究结果的比较，希望最终聚焦到两个衰变源实验方案，从而为未来开展吨级规模实验做好启动规划和前期预研建议。

围绕无中微子双贝塔衰变实验，该咨询项目将主要产生三项研究成果：一本书（“中国学科发展战略”丛书之一）、一份战略报告以及一篇科普文章。

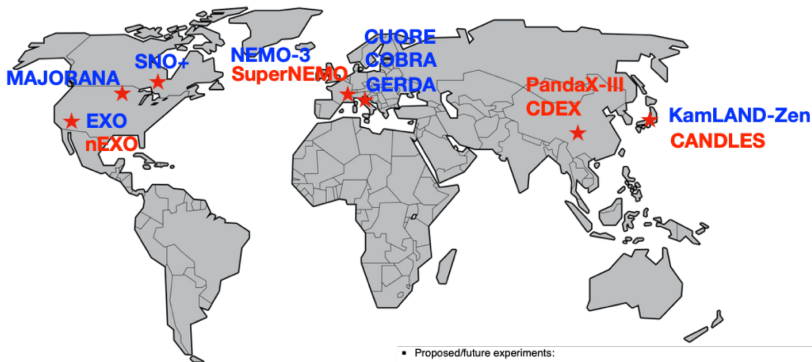
无中微子双贝塔衰变实验是测定中微子质量最好的方法，不仅可以确定中微子是Majorana费米子，还可以确定中微子的反粒子就是它本身。通过无中微子双贝塔衰变实验，可以揭示出轻子数守恒破坏以及宇宙物质的非对称性等规律，因此该实验具有重大的科学意义。沈文庆院士、张宗燧院士、罗民兴院士、马余刚院士、锦屏地下实验室主任程建平，以及各个实施方案主要代表、相关领域专家、中科院数理学部有关负责人参加了首次研讨会。会上，张焕乔院士强调了无中微子双贝塔衰变的科学意义和实验探测难度，概述了国内的实验研究现状，并指明了本次研讨会的目的。

来自复旦大学、清华大学、中科院近代物理研究所、上海交通大学四个实施方案的代表分别介绍了各自实验研究的特点、难点及已经取得的成果和发展路线。核工业工程研究院、北京大学和中科院高能物理研究所有关专家分别介绍了国内同位素分离有关情况及相关理论研究情况。

与会专家围绕相关探测技术、同位素和可能的灵敏度极限等问题进行了热烈讨论，就如何发挥各实验室优势、节省科研经费并提高研发效率、加强合作以提升整体水平等方面达成共识，并建议可考虑通过与粒子物理和能量学领域的学者建立密切、开放的联系。

Canada, Japan, European countries?

Worldwide experiments running and proposed



Experiments taking data as of November 2017:

- COBRA, ^{116}Cd in room temperature CdZnTe crystals
- CUORE, ^{130}Te in ultracold TeO_2 crystals
- EXO, a ^{136}Xe and ^{134}Xe search
- GERDA, a ^{76}Ge detector
- KamLAND-Zen, a ^{136}Xe search. Data collection from 2011.^[21]
- MAJORANA, using high purity ^{76}Ge p-type point-contact detectors.^[22]

Proposed/future experiments:

- CANDELS, ^{48}Ca in CaF_2 , at Kamioka Observatory
- MOON, developing ^{100}Mo detectors
- AMoRE, ^{100}Mo enriched CaMoO_4 crystals at YangYang underground laboratory^[23]
- nEXO, using liquid ^{136}Xe in a time projection chamber^[24]
- LEGEND, Neutrinoless Double-beta Decay of ^{76}Ge .
- LUMINEU, exploring ^{100}Mo enriched ZnMoO_4 crystals at LSM, France.
- NEXT, a Xenon TPC. NEXT-DEMO ran and NEXT-100 will run in 2016.
- SNO+, a liquid scintillator, will study ^{130}Te
- SuperNEMO, a NEMO upgrade, will study ^{82}Se
- TIN.TIN, a ^{124}Sn detector at INO
- PandaX-III, an experiment with 200 kg to 1000 kg of 90% enriched ^{136}Xe

source: https://en.wikipedia.org/wiki/Double_beta_decay

Experimental sensitivity

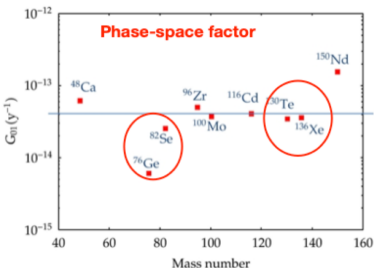
$$(T_{1/2}^{0\nu}) \propto \begin{cases} a M \varepsilon t & \text{background free,} \\ a \varepsilon \sqrt{\frac{M t}{B \Delta E}} & \text{with background,} \end{cases}$$

mass of the source
isotopic abundance of the parent isotope
detection efficiency of the signal in the ROI
measurement time
background index
detector energy resolution

Isotope	Natural abundance (%)	$Q_{\beta\beta}$ (MeV)
⁴⁸ Ca	0.187	4.263
⁷⁶ Ge	7.8	2.039
⁸² Se	8.7	2.998
⁹⁶ Zr	2.8	3.348
¹⁰⁰ Mo	9.8	3.035
¹¹⁶ Cd	7.5	2.813
¹³⁰ Te	34.08	2.527
¹³⁶ Xe	8.9	2.459
¹⁵⁰ Nd	5.6	3.371

Michelle J. Dolinski et al (2019)

Isotope	$T_{1/2}^{0\nu} (\times 10^{25} \text{ y})$	$\langle m_{\beta\beta} \rangle (\text{eV})$	Experiment
⁴⁸ Ca	$> 5.8 \times 10^{-3}$	$< 3.5 - 22$	ELEGANT-IV
⁷⁶ Ge	> 8.0	$< 0.12 - 0.26$	GERDA
	> 1.9	$< 0.24 - 0.52$	MAJORANA DEMO
⁸² Se	$> 3.6 \times 10^{-2}$	$< 0.89 - 2.43$	NEMO-3
⁹⁶ Zr	$> 9.2 \times 10^{-4}$	$< 7.2 - 19.5$	NEMO-3
¹⁰⁰ Mo	$> 1.1 \times 10^{-1}$	$< 0.33 - 0.62$	NEMO-3
¹¹⁶ Cd	$> 1.0 \times 10^{-2}$	$< 1.4 - 2.5$	NEMO-3
¹²⁸ Te	$> 1.1 \times 10^{-2}$	—	—
¹³⁰ Te	> 1.5	$< 0.11 - 0.52$	CUORE
¹³⁶ Xe	> 10.7	$< 0.061 - 0.165$	KamLAND-Zen
	> 1.8	$< 0.15 - 0.40$	EXO-200
¹⁵⁰ Nd	$> 2.0 \times 10^{-3}$	$< 1.6 - 5.3$	NEMO-3



Experimental sensitivity (currently best)



Isotope	Experiment	Exposure (kg yr)	$T_{1/2}^{0\nu\beta\beta}$ average sensitivity (10^{25} yr)	$T_{1/2}^{0\nu\beta\beta}$ (10^{25} yr) 90%CL	$\langle m_\nu \rangle$ (meV) Range from NME*	Reference
^{76}Ge	GERDA	82.4	11	>9.0	<113-254	Agostini et al. PRL 120 (2018) 132503
	MJD	29.7	4.8	>2.7	<200-433	Alvis et al. arXiv:1902.02299 (2019)
^{130}Te	CUORE	24.0	0.7	>1.5	<110-520	Alduino et al. PRL 120 (2018) 132501
^{136}Xe	EXO-200	234.1	5.0	>3.5	<93-286	Anton et al. arXiv:1906.02723 (2019)
	KamLAND-ZEN	504	5.6	>10.7	<60-161	Gando et al., PRL 117 (2016) 082503

Michelle Dolinski, ECT* workshop (2019)

What can we contribute from nuclear-structure community?



■ The NME governing this process

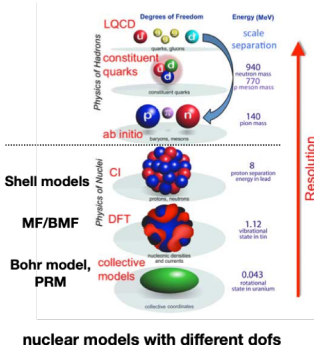
$$M^{0\nu}(0_I^+ \rightarrow 0_F^+) = \langle 0_F^+ | O^{0\nu} | 0_I^+ \rangle$$

where the transition operator in the exchange of light neutrinos

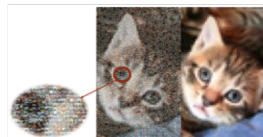
$$\begin{aligned} O^{0\nu} &= \frac{4\pi R}{g_A^2} \int d^3\vec{r}_1 \int d^3\vec{r}_2 \int \frac{d^3\vec{q}}{(2\pi)^3} \\ &\times \frac{e^{i\vec{q}\cdot(\vec{r}_1 - \vec{r}_2)}}{q(q + E_d)} \mathcal{J}_\mu^\dagger(\vec{r}_1) \mathcal{J}^{\mu\dagger}(\vec{r}_2) \end{aligned}$$

where the effective nuclear current is chosen as

$$\begin{aligned} \mathcal{J}_\mu^\dagger(x) &= \bar{\psi}(x) \left[g_V(q^2) \gamma_\mu - g_A(q^2) \gamma_\mu \gamma_5 \right. \\ &\quad \left. + ig_M(q^2) \frac{\sigma_{\mu\nu}}{2m_p} q^\nu - g_P(q^2) q_\mu \gamma_5 \right] \tau^+ \psi(x). \end{aligned}$$



nuclear models with different dofs



Short-distance physics seems NOT important for nuclear low-lying states

What can we contribute in nuclear-structure community?



$$O^{0\nu} = \frac{2R}{\pi g_A^2} \int_0^\infty q dq \sum_{a,b} \frac{j_0(qr_{ab})[h_F(q) + h_{\text{GT}}(q)\vec{\sigma}_a \cdot \vec{\sigma}_b] + j_2(qr_{ab})h_T(q)[3\vec{\sigma}_j \cdot \hat{r}_{ab}\vec{\sigma}_k \cdot \hat{r}_{ab} - \vec{\sigma}_a \cdot \vec{\sigma}_b]}{q + \bar{E} - (E_i + E_f)/2} \tau_a^+ \tau_b^+$$

$$h_{F\text{-VV}}(q^2) = -g_V^2(q^2),$$

$$h_{\text{GT-AA}}(q^2) = -g_A^2(q^2),$$

$$h_{\text{GT-AP}}(q^2) = \frac{2}{3}g_A(q^2)g_P(q^2)\frac{q^2}{2m_p},$$

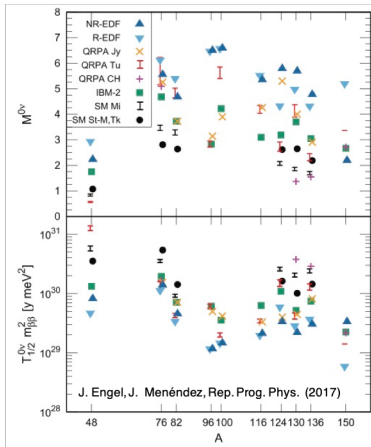
$$h_{\text{GT-PP}}(q^2) = -\frac{1}{3}g_P^2(q^2)\frac{q^4}{4m_p^2},$$

$$h_{\text{GT-MM}}(q^2) = -\frac{2}{3}g_M^2(q^2)\frac{q^2}{4m_p^2},$$

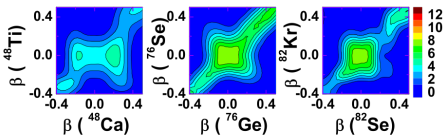
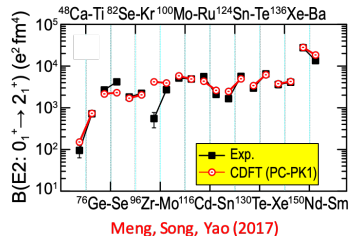
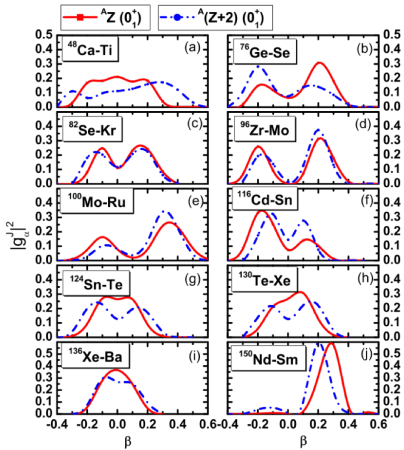
$$h_{T\text{-AP}}(q^2) = h_{\text{GT-AP}}(q^2),$$

$$h_{T\text{-PP}}(q^2) = h_{\text{GT-PP}}(q^2),$$

$$h_{T\text{-MM}}(q^2) = -\frac{1}{2}h_{\text{GT-MM}}(q^2).$$



Impact of collective correlations on the NMEs for $0\nu\beta\beta$ decay



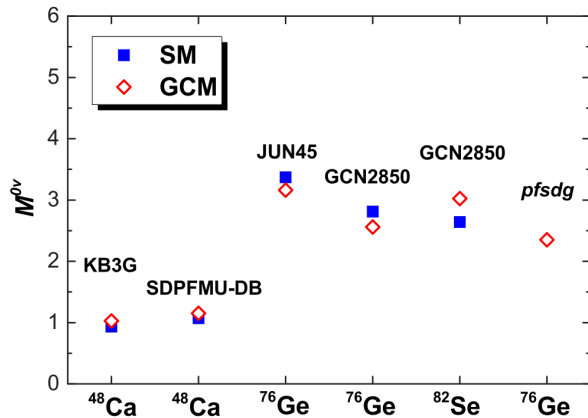
Song, JMY, Ring, Meng (2014)
JMY, Song, Hagino, Ring, Meng (2015)

	^{48}Ca	^{48}Ti	NME (F/GT/T)
spherical	-7.558	-20.497	-2.276/4.736/0.116
GCM:Q ₂₀	-7.670	-23.556	-0.231/0.903/0.024
GCM:Q ₂₀ +T=1	-7.855	-24.198	-0.236/1.415/0.058
GCM:Q ₂₀ +T=1+T=0	-	-24.467	-0.241/0.888/0.057
SM seniority 0	-7.578	-20.507	-2.287/4.783/0.116
SM full	-7.959	-24.896	-0.234/0.886/0.057

- GCM and Shell Model calculations have been performed in the *pf*-shell with KB3G interactions both!
- Variational approach to SM results with GCM approaches is evident.
- Almost perfect agreement between SM seniority 0 and PN-VAP spherical calculations

Courtesy of T. R. Rodríguez

Shell Model vs GCM



Jiao, Engel, Holt (2017)

ab initio calculations of atomic nuclei



- Remarkable progress achieved in *ab initio* calculations of atomic nuclei starting from modern nuclear interactions

NCSM, Lattice MC, VMC,
GFMC, SCGF, **IMSRG**,
(B)CC, MBPT, (R)BHF,
etc

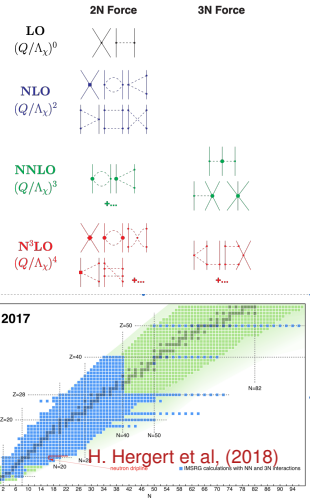
- Great success of applying renormalization-group methods into nuclear many-body calculations (free-space SRG and in-medium SRG)

IN-NCSM, EOM-IMSRG,
VS-IMSRG, etc

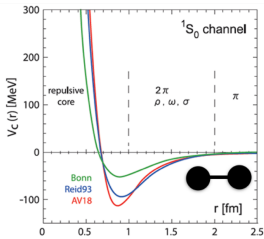
- *No-core* calculation of medium-mass open-shell nuclei with strong collective correlations is still a challenge.

IMSRG+GCM, m-scheme
CC, etc.

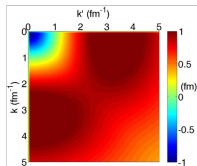
R. Machleidt, D. R. Entem (2011)



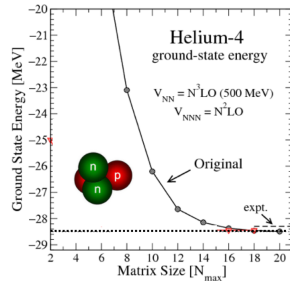
Challenges in the *ab initio* calculations of atomic nuclei



$$V_{\ell=0}(k, k') = \int d^3r j_0(kr) V(r) j_0(k'r)$$



S. Bogner et al., PPNP (2010)

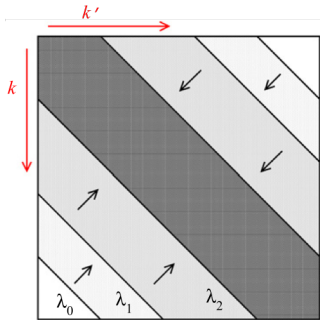


- Repulsive core & strong tensor force => low and high k modes strongly coupled by the interaction
- non-perturbative, poorly convergent basis expansions (cutoff Λ , No. of s.p. states D)

$$\text{Dim}(H) \sim \frac{D!}{(D-A)!A!}, \quad D \sim \Lambda^3 A$$

For $\Lambda = 4.0 \text{ fm}^{-1}$, $A = 16$, $\text{Dim}(H) \sim 10^{14}$.

Similarity RG evolution of nucleon-nucleon interaction



The flow parameter s is usually replaced with $\lambda = s^{-1/4}$ with units of fm^{-1} .

S. K. Bogner, R. J. Furnstahl, and
R. J. Perry (2007)

- Apply unitary transformations to Hamiltonian

$$H_s = U_s H U_s^\dagger \equiv T_{\text{rel}} + V_s \quad (1)$$

- Flow equation

$$\frac{dH_s}{ds} = [\eta_s, H_s], \quad (2)$$

where the generator η_s is chosen to diagonalize $H(s)$ in the eigenbasis of T_{rel} ,

$$\eta_s = [T_{\text{rel}}, H_s] \quad (3)$$

$$\begin{aligned} \frac{dV_s(k, k')}{ds} &= -(k^2 - k'^2) V_s(k, k') \\ &+ \frac{2}{\pi} \int_0^\infty q^2 dq (k^2 + k'^2 - 2q^2) V_s(k, q) V_s(q, k') \end{aligned}$$

Similarity RG evolution of nucleon-nucleon interaction

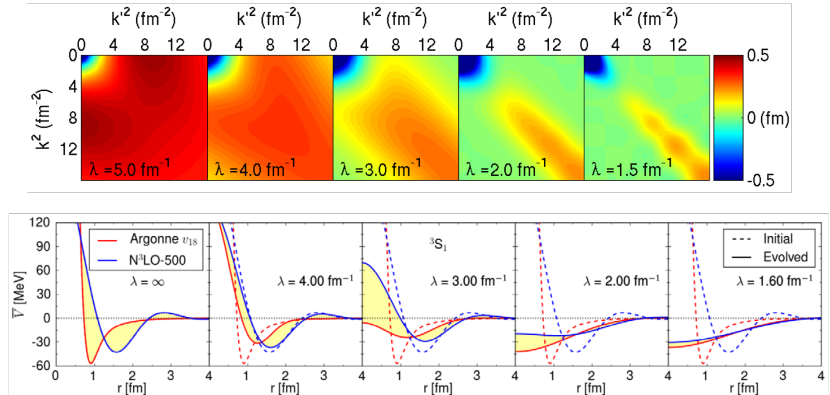
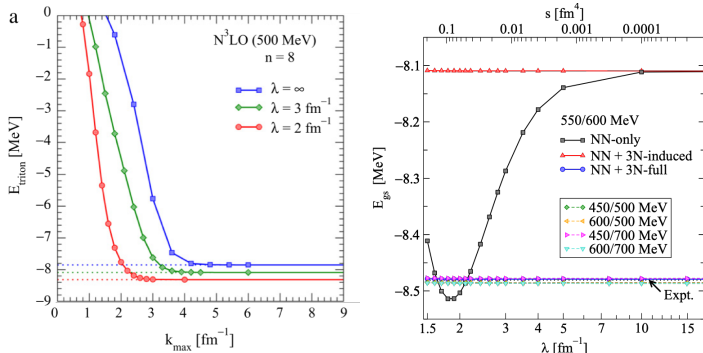


Figure: Local projection of AV18 and $N^3LO(500$ MeV) potentials $V(r)$ in 3S_1 channel.

- “Hard core” disappears in the softened interactions
- S. K. Bogner et al. (2010); Wendt et al. (2012)

Similarity RG evolution of nucleon-nucleon interaction



- Convergence becomes faster as the decreases of the λ (resolution/degree of decoupling).
- importance of (induced) three-body forces

Bogner et al. (2008); Furnstahl et al. (2013)

Many-body methods: No-core shell model

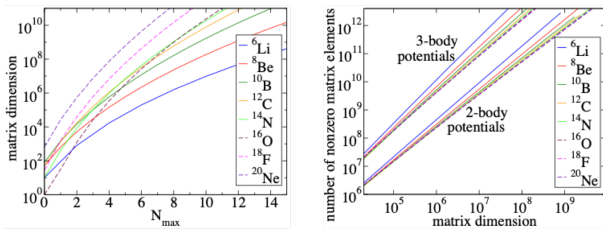
- The A-body Schroedinger equation

$$H|\Psi\rangle = E|\Psi\rangle,$$

- The wave function is expanded in terms of many-body basis states

$$|\Psi\rangle = \sum_{\mu} c_{\mu} |\Phi_{\mu}\rangle,$$

where c_{μ} is to be determined from the diagonalization of the H . $|\Phi_{\mu}\rangle$ is a Slater Determinant of single-particle states occupied by the nucleons.



from: C. Yang, H. M. Aktulga, P. Maris, E. Ng, J. Vary, Proceedings of NTSE-2013

The IMSRG in a nutshell

- A set of continuous **unitary transformations** onto the Hamiltonian

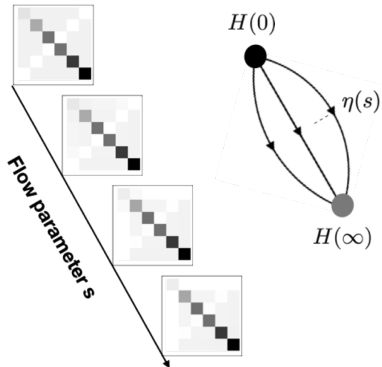
$$H(s) = U(s)H_0U^\dagger(s)$$

- Flow equation for the Hamiltonian

$$\frac{dH(s)}{ds} = [\eta(s), H(s)]$$

where the $\eta(s) = \frac{dU(s)}{ds}U^\dagger(s)$ is the so-called generator chosen to decouple a given **reference state** from its excitations.

- Computation complexity scales **polynomially** with nuclear size

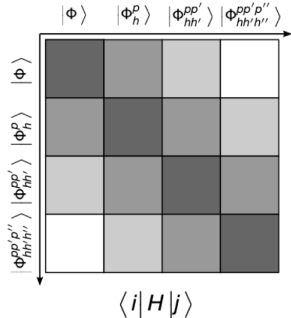


Tsukiyama, Bogner, and Schwenk (2011)

Hergert, Bogner, Morris, Schwenk, Tsukiyama (2016)

Not necessary to construct the H matrix elements in many-body basis !

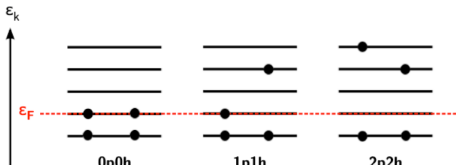
The IMSRG for closed-shell nuclei



- reference state: **single Slater determinant**

Normal-Ordered Hamiltonian

$$H = E_0 + \sum_{kl} f_l^k : A_l^k : + \frac{1}{4} \sum_{klmn} \Gamma_{mn}^{kl} : A_{mn}^{kl} : + \frac{1}{36} \sum_{ijklmn} W_{lmn}^{ijk} : A_{lmn}^{ijk} :$$



excitations relative
to reference state:
normal-ordering

$$\langle \overset{\textcolor{red}{p}}{h} | H | \Psi \rangle = \sum_{kl} f_l^k \langle \Psi | : A_p^h :: A_l^k : | \Psi \rangle = -n_h \bar{n}_p f_h^p$$

$$\langle \overset{\textcolor{red}{pp'}}{hh'} | H | \Psi \rangle = \sum_{klmn} \Gamma_{mn}^{kl} \langle \Psi | : A_{pp'}^{hh'} :: A_{mn}^{kl} : | \Psi \rangle \sim \Gamma_{hh'}^{pp'}$$

Courtesy of Heiko Hergert

Strategies for open-shell nuclei with strong collective correlations



1 SR-IMSRG with high-rank operators

$$|\Phi_{\text{ref}}\rangle \sim |\Phi_0(\text{HF})\rangle,$$

$$\hat{O} = \sum_{a,i} O_i^a A_i^a + \sum_{ab,ij} O_{ij}^{ab} A_{ij}^{ab} + \sum_{abc,ijk} O_{ijk}^{abc} A_{ijk}^{abc} + \dots$$

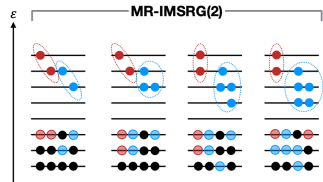
2 MR-IMSRG with low-rank operators

$$|\Phi_{\text{ref}}\rangle \sim (1 + c_i^a A_i^a + c_{ij}^{ab} A_{ij}^{ab} + c_{ijk}^{abc} A_{ijk}^{abc} + \dots) |\Phi_0\rangle$$

$$\hat{O} = \sum_{a,i} O_i^a A_i^a + \sum_{ab,ij} O_{ij}^{ab} A_{ij}^{ab}$$

IM-NCSM: Gebrerufael, Vobig, Hergert, Roth (2017)

Reference state matters in the truncated IMSRG



MR-IMSRG: build correlations on top of already correlated state (e.g., from a method that describes static correlation well)



Source: National Geographic; Peer research

Jeff Guntens, The Denver Post

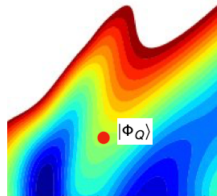
The IMSRG+GCM method: the reference state



Thouless' theorem

Any other general (symmetry broken) product wave function $|\Phi_Q\rangle$ which is not orthogonal to $|\Phi_0\rangle$ may be expressed as

$$|\Phi_Q\rangle \propto \exp\left(\sum_{pq} Z_{pq}^{(Q0)} \alpha_p^\dagger \alpha_q^\dagger\right) |\Phi_0\rangle, \quad \alpha_p^\dagger = U_{qp}^* a_q^\dagger + V_{qp} a_q$$



- The multi-reference state can be rewritten as

$$\begin{aligned} |\Phi_{\text{ref}}\rangle &= \hat{P}^J \hat{P}^N \hat{P}^Z \sum_Q F_Q |\Phi_Q\rangle \\ &\sim (1 + c_i^a A_i^a + c_{ij}^{ab} A_{ij}^{ab} + c_{ijk}^{abc} A_{ijk}^{abc} + \dots) |\Phi_0\rangle \end{aligned}$$

- \hat{P} s are projection operators.
- F_Q is determined with variational principles.
- $\{|\Phi_Q\rangle\}$ forms a set of basis for nuclear collective correlated states with Q being called generator coordinate.

- The trial wave function of a GCM state (serving as the reference state of IMSRG):

$$|\Phi_{\text{ref}}^{JNZ}\rangle = \sum_Q F_Q^{JNZ} \hat{p}^J \hat{p}^N \hat{p}^Z |\Phi_Q\rangle$$

$|\Phi_Q\rangle$ are a set of HFB wave functions from constraint calculations.

- The mixing weight $F^{JNZ}(q_i)$ is determined with variational principle, leading to the Hill-Wheeler-Griffin equation:

$$\sum_{Q'} \left[H^{JNZ}(Q, Q') - E^J N^{JNZ}(Q, Q') \right] F_{Q'}^{JNZ} = 0$$

Features of GCM

- The Hilbert space in which the H will be diagonalized is defined by the Q .
Many-body correlations are controlled by the Q
- The Q is chosen as (collective) degrees of freedom relevant to the physics.
- Dimension of the space in GCM is generally much smaller than full CI calculations.

The IMSRG+GCM method: normal-ordering

- For a given general Hamiltonian, we normal-order it with respect to the GCM reference state H. Hergert et al. (2017)

$$H = E^{(0b)}(\lambda) + f^{(1b)}(\lambda) + \Gamma^{(2b)}(\lambda) + W^{(3b)}(\lambda) + \dots$$

where collective correlations are encoded in the **irreducible** many-body density matrices

$$\begin{aligned}\lambda_q^p &= \rho_q^p, \\ \lambda_{rs}^{pq} &= \rho_{rs}^{pq} - \mathcal{A}(\lambda_r^p \lambda_s^q), \\ \color{red} \lambda_{stu\dots}^{pqr\dots} &= \rho_{stu\dots}^{pqr\dots} - \mathcal{A}(\lambda_s^p \lambda_{tu\dots}^{qr\dots}) - \dots - \mathcal{A}(\lambda_s^p \lambda_t^q \lambda_u^r \dots),\end{aligned}$$

with $\rho_{stu\dots}^{pqr\dots} = \langle \Phi_{\text{ref}} | A_{stu\dots}^{pqr\dots} | \Phi_{\text{ref}} \rangle$.

General hierarchy in the contribution: $\lambda^{(1b)} >> \lambda^{(2b)} >> \lambda^{(3b)} >> \dots$

WARNING

Computation of the k -body density matrices with rank $k \geq 3$ for deformed nuclei in a large (full) model space is a difficult task.

The IMSRG+GCM method: procedure



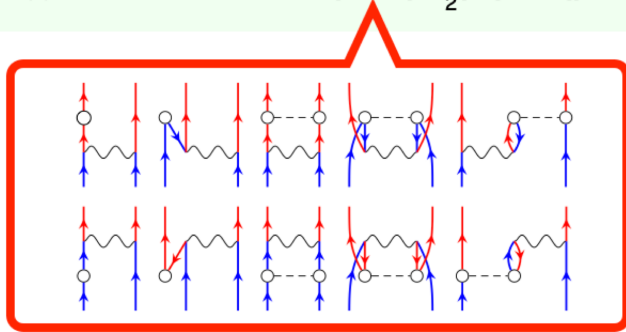
$0\nu\beta\beta$ decay operator in IMSRG(2)



$$O^{0\nu} = \frac{4\pi R}{g_A^2} \int d^3\vec{r}_1 \int d^3\vec{r}_2 \int \frac{\int d^3\vec{q}}{(2\pi)^3} \frac{e^{i\vec{q}\cdot(\vec{r}_1-\vec{r}_2)}}{q(q+E_d)} \mathcal{J}_\mu^\dagger(\vec{r}_1) \mathcal{J}^{\mu\dagger}(\vec{r}_2)$$

$0\nu\beta\beta$ transition operator in IMSRG(2)

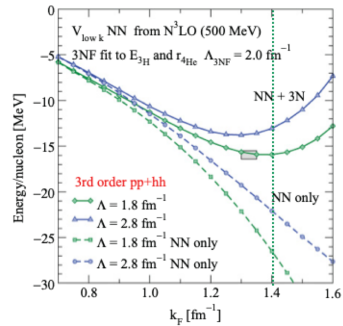
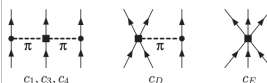
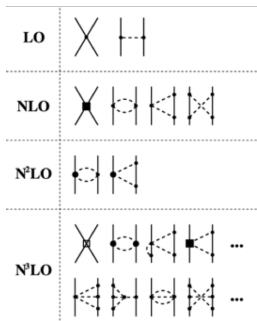
$$O^{0\nu}(s) \equiv e^{\Omega(s)} O^{0\nu} e^{-\Omega(s)} = O^{0\nu} + [\Omega, O^{0\nu}] + \frac{1}{2} [\Omega, [\Omega, O^{0\nu}]] + \dots$$



The IMSRG+GCM: implementation of chiral 2N+3N interactions

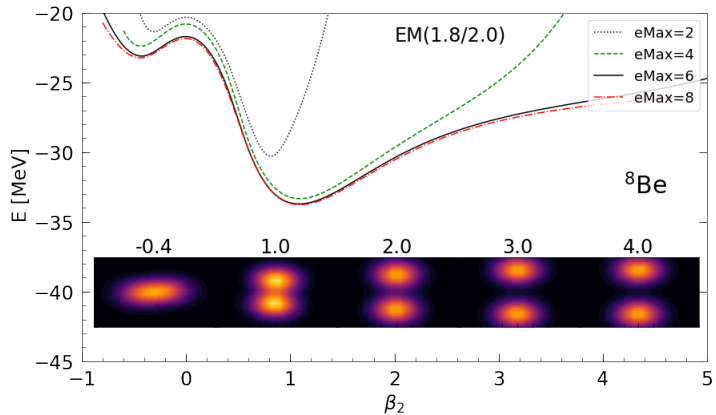


$$H = \sum_{i < j} \frac{(\mathbf{p}_i - \mathbf{p}_j)^2}{2mA} + \sum_{i < j} V_{ij}^{(2)} + \sum_{i < j < k} V_{ijk}^{(3)}$$



Hebeler et al., PRC83, 031301(R) (2011)

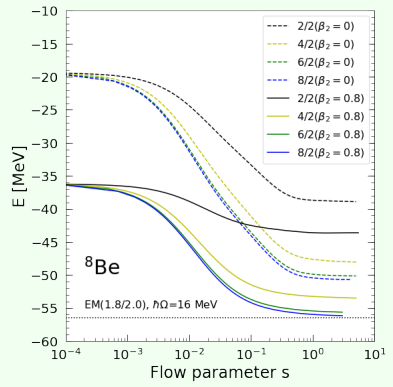
Application: two-alpha cluster structure in ${}^8\text{Be}$



- HFB potential energy surface by the SRG softened chiral interaction
EM1.8/2.0($\hbar\Omega = 16$ MeV)

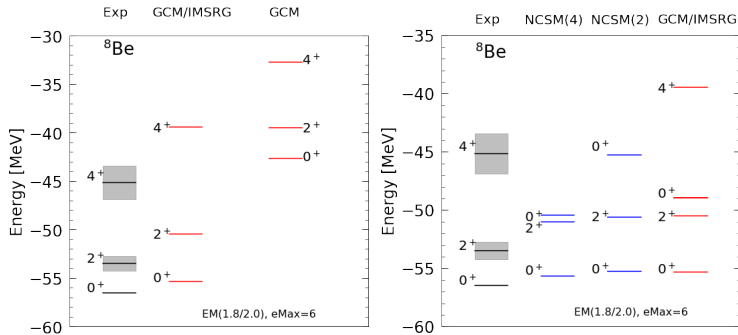
Application: two-alpha cluster structure in ${}^8\text{Be}$

Energy flow



- Starting from the spherical or two- α cluster state, the IMSRG(2) is converged to different 0^+ states.

Application: two-alpha cluster structure in ${}^8\text{Be}$



- Low-lying states by pure GCM and IMSRG+GCM
- Low-lying states by IMSRG+GCM and IMSRG+NCSM

Application: $0\nu\beta\beta$ from ^{22}O to ^{22}Ne

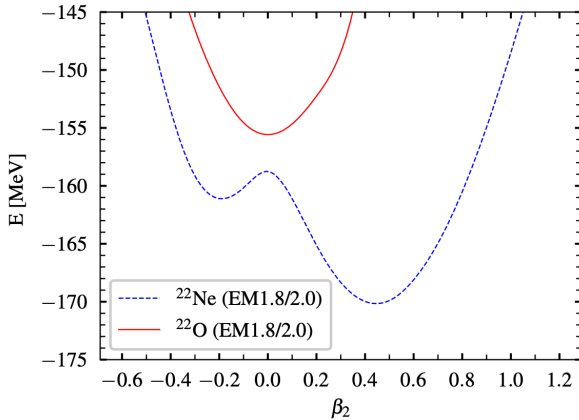
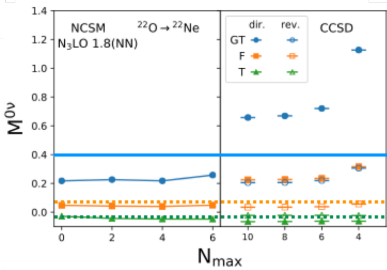
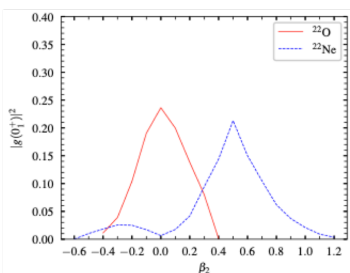
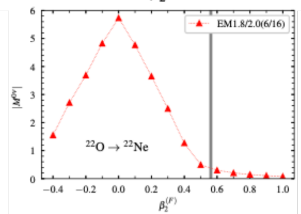
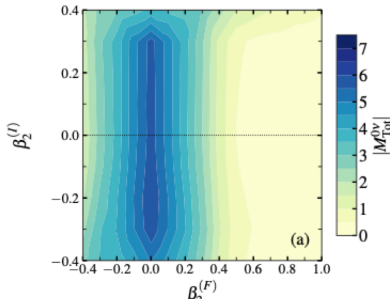
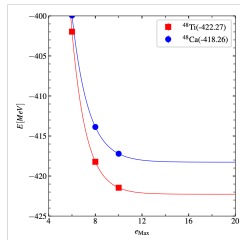
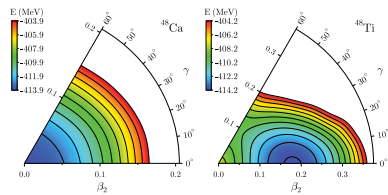
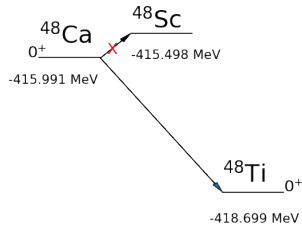


Figure: The potential energy surface from VAP+PNP (HFB) calculation with $e_{\text{Max}} = 6$, $\hbar\Omega = 16$ MeV.

Application: $0\nu\beta\beta$ from ^{22}O to ^{22}Ne



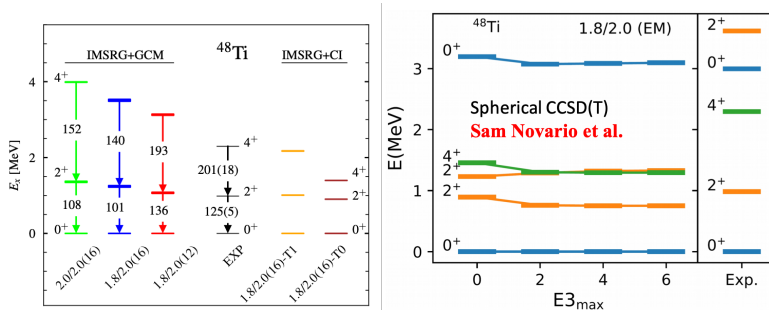
Application: $0\nu\beta\beta$ from ^{48}Ca to ^{48}Ti



- An ensemble reference state

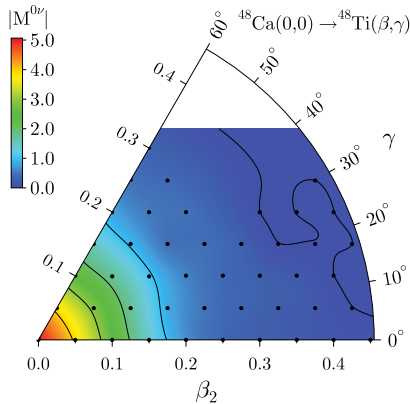
$$\rho = \alpha |^{48}\text{Ca}\rangle\langle^{48}\text{Ca}| + (1-\alpha)|^{48}\text{Ti}\rangle\langle^{48}\text{Ti}|$$

Application: $0\nu\beta\beta$ from ^{48}Ca to ^{48}Ti



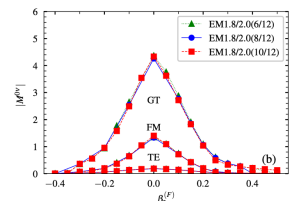
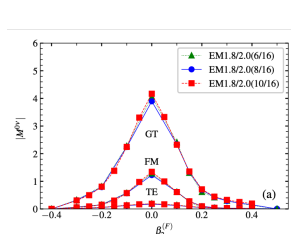
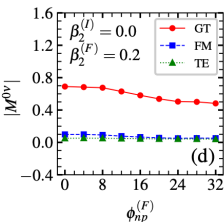
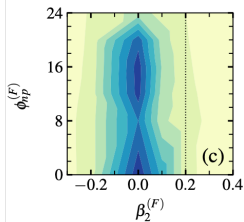
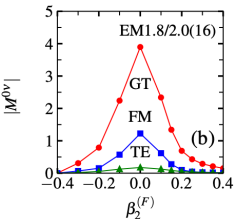
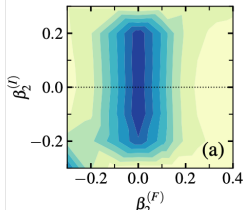
- Low-energy structure of ^{48}Ti by IMSRG+GCM is reasonably reproduced (spectrum stretched).
- Inclusion of non-collective configurations from neutron-proton isoscalar pairing fluctuation in IMSRG+GCM compresses the spectra by about 6%.
- The spectra by the spherical CCSD(T) seems to be close to results by the IMSRG+CI(T0)
- With more collective correlations in the IMSRG+CI, the spectrum becomes more stretched.

Application: $0\nu\beta\beta$ from ^{48}Ca to ^{48}Ti



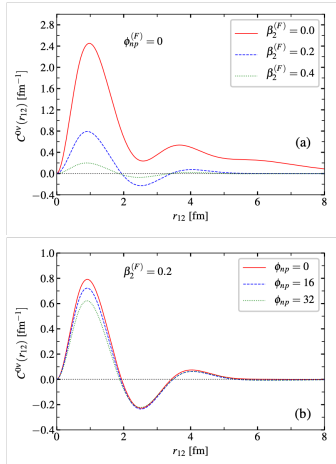
- The triaxiality γ -dependence of the $M^{0\nu}$ is very weak.

Application: $0\nu\beta\beta$ from ^{48}Ca to ^{48}Ti



- The $M^{0\nu}$ is decreasing dramatically with the deformation of ^{48}Ti
- The $M^{0\nu}$ is moderately decreasing with ϕ_{np} in ^{48}Ti

Application: $0\nu\beta\beta$ from ^{48}Ca to ^{48}Ti



$$M^{0\nu} = \int dr_{12} C^{0\nu}(r_{12})$$

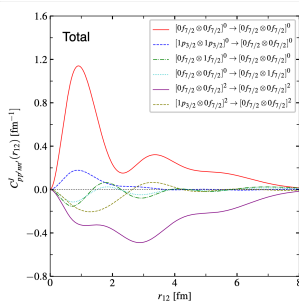
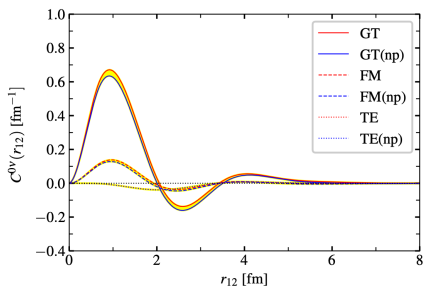
- The quadrupole deformation in ^{48}Ti changes both the short and long-range behaviors
- Neutron-proton isoscalar pairing is a short-range effect

Application: $0\nu\beta\beta$ from ^{48}Ca to ^{48}Ti

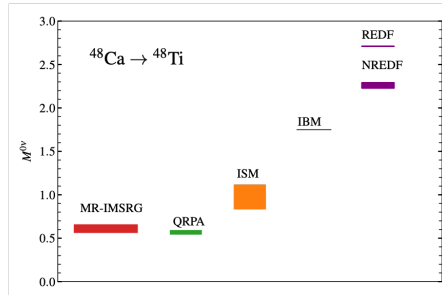
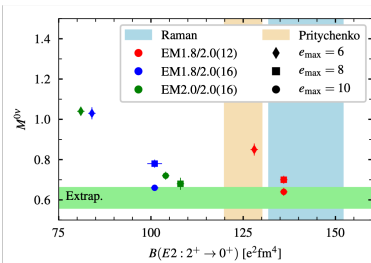
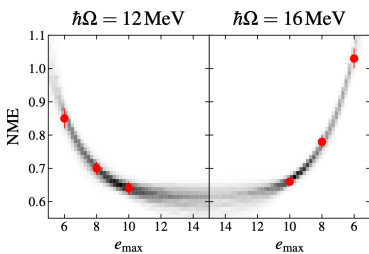
$$C^{0\nu}(r_{12}) = \sum_{p \leq p', n \leq n'} \cdot \sum_J C_{pp' nn'}^J(r_{12}),$$

with

$$C_{pp' nn'}^J(r_{12}) = \frac{(2J+1)}{\sqrt{(1+\delta_{pp'})(1+\delta_{nn'})}} \langle (pp')J | \bar{O}^{0\nu}(r_{12}) | (nn')J \rangle \rho_{pp' nn'}^J,$$



Application: $0\nu\beta\beta$ from ^{48}Ca to ^{48}Ti (preliminary results)



- The value from Markov-chain Monte-Carlo extrapolation is $M^{0\nu} = 0.61^{+0.05}_{-0.04}$
- The neutron-proton isoscalar pairing fluctuation quenches $\sim 17\%$ further, which might be canceled out partially by the isovector pairing fluctuation.

Taking-away messages:

- Worldwide ton-scale experiments are proposed to measure the $0\nu\beta\beta$ from which the determination of neutrino mass relies on the NMEs.
- Several groups have begun programs to calculate the NMEs from first principles, taking advantage of a flowering of ab initio nuclear-structure theory in the last couple of decades.
- The multi-reference IMSRG+GCM opens a door to modeling deformed nuclei with realistic nuclear forces (from chiral EFT). Many interesting phenomena of low-energy physics (shape transition, coexistence, cluster structure) can be explored within this framework.
- The NME from $^{48}\text{Ca} \rightarrow ^{48}\text{Ti}$ is calculated from *first principles*.

What's next:

- Extension to heavier candidate nuclei, like $^{76}\text{Ge} \rightarrow ^{76}\text{Se}$ and $^{136}\text{Xe} \rightarrow ^{136}\text{Ba}$.
- More benchmarks among several different *ab initio* methods for the NMEs.
- Quantification of uncertainties from different sources.

Collaborators and acknowledgement

Michigan State University

- Scott Bogner
- Heiko Hergert
- Roland Wirth

San Diego State University

- Changfeng Jiao

Universidad Autónoma de Madrid

- Tomás R. Rodríguez

Southwest University

- Longjun Wang

Peking University

- Jie Meng
- Peter Ring
- Lingshuang Song

University of North Carolina at Chapel Hill

- Benjamin Bally
- Jonathan Engel

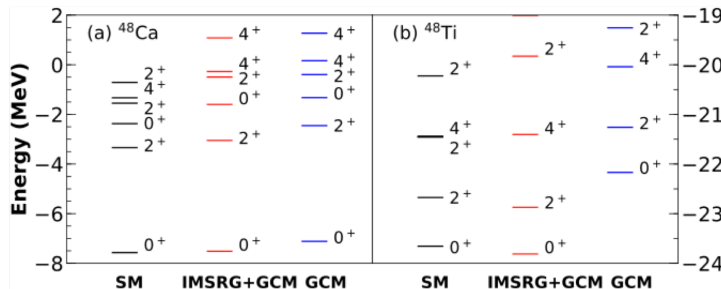
Iowa State University

- Robert A. Basili
- James P. Vary

The IMSRG+GCM method: a benchmark calculation



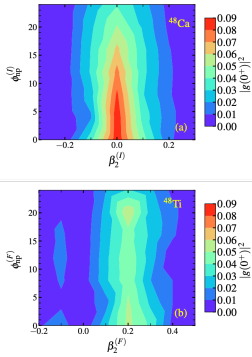
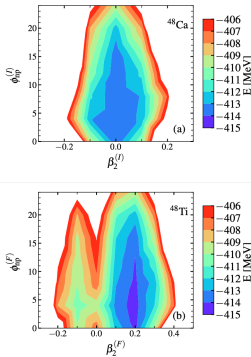
In valence-space *pf* shell, many-body density matrices of a multi-reference state can be calculated without difficulty.



JMY. J. Engel, L.J. Wang, C.F. Jiao, H. Hergert (2018)

The IMSRG overall improves the agreement with the shell-model results.

Application: $0\nu\beta\beta$ from ^{48}Ca to ^{48}Ti



- The np isoscalar pairing amplitude:

$$\phi_{np} = \langle \Phi | P_0^\dagger | \Phi \rangle + \langle \Phi | P_0 | \Phi \rangle$$

with

$$P_\mu^\dagger = \frac{1}{\sqrt{2}} \sum_\ell \hat{\ell} [a_\ell^\dagger a_\ell^\dagger]_{0\mu 0}^{L=0, J=1, T=0}$$

- Collective wave functions of g.s. extended along the ϕ_{np} .

Early researches on nuclear single beta-decay



- 1914, Chadwick established the continuous feature of the kinetic energy spectrum of the beta-decay electron

$$^A Z \rightarrow ^A (Z + 1) + e^- + ?$$

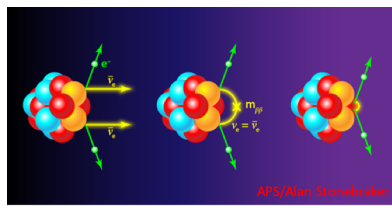
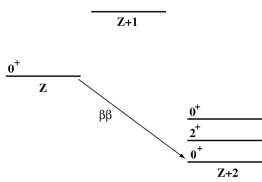


- 1930, Pauli suggested the emission of an additional spin-1/2, weakly-interacting neutral particle ($? = \bar{\nu}_e$)
- 1934, Fermi published the four-fermion theory of beta decay

$$\mathcal{L}_{\text{Fermi}} = -\frac{G_F}{\sqrt{2}} (\bar{\rho} \gamma_\mu n)(\bar{e} \gamma^\mu \nu) + h.c.$$

Early researches on double beta-decay

- 1935, Goeppert-Mayer discussed the $2\nu\beta\beta$ decay based on the Fermi theory ($T_{1/2}^{2\nu} > 10^{17}$ y)
Goeppert-Mayer, Phys. Rev. 48, 512 (1935)
- 1937, Majorana formulated a theory of neutrinos in which there was no distinction between neutrinos and antineutrinos
E. Majorana, Nuovo Cimento 14, 171 (1937).
- 1939, Furry discussed the transition probability of $0\nu\beta\beta$ decay based on the Fermi theory and massless neutrino ($\sim 10^5$ faster than $2\nu\beta\beta$ decay for $Z = 31$ due to different phase space factors)
W. Furry, Phys. Rev. 56, 1184 (1939)



- 1956, Lee and Yang questioned the conservation law of parity in weak interaction (confirmed by the Wu experiment in 1957).
- 1957, Salam, Landau, Lee and Yang formulated the theory of a massless two-component neutrinos with definite helicity.
- 1958, Feynman and Gell-Mann, Sudarshan and Marshak proposed the V-A theory of the weak interaction



$$\mathcal{L}_{V-A} = -\frac{G_F}{\sqrt{2}} \bar{\rho} \gamma_\mu (1 - \gamma_5) n \bar{e} \gamma^\mu (1 - \gamma_5) \nu + h.c.$$

Impacts on the $0\nu\beta\beta$

- The $V - A$ weak interaction implies the presence of an additional chiral selection, blocking the $0\nu\beta\beta$ decay ($\Gamma^{0\nu} \ll \Gamma^{2\nu}$).
- 1960, Greuling and Whitten calculated the probability of $0\nu\beta\beta$ under the assumption of (i) the existence of the Majorana mass of the neutrino ($\Gamma^{0\nu} \propto m_\nu^2$ if $m_\nu \neq 0$), or (2) a small violation δ of $V - A$ interaction.
- In 1960s, the sensitivity $T_{1/2}^{0\nu} > 10^{21}$ yr was achieved in experiments with ^{48}Ca , ^{76}Ge , and ^{82}Se by E. Fiorini, C. Wu, T. Kirsten, and O. Manuel.

Revival of neutrinoless double beta decay



- 1980, Lubimov claimed the detection of a neutrino mass of ~ 30 eV in the measurement of β spectrum of tritium (not confirmed). These neutrinos were considered as a candidate for dark matter in cosmology.
- 1981, A new type of $0\nu\beta\beta$ decay was considered by Chikashige, Aulakh, Gelmini, Georgi, et al

$$^A Z \rightarrow ^A (Z + 2) + 2e + \chi^0$$

where χ^0 is a massless Goldstone boson (called Majoron) appearing under the global breakdown of the $B - L$ symmetry.

- The Schechter-Valle theorem states that any diagram causing $0\nu\beta\beta$ decay will generate a Majorana mass term for light neutrinos, which renders them Majorana particles [Schechter, Valle \(1982\)](#).
- 1998-2003, the discovery of massive neutrinos through the observation of neutrino oscillations suggests the existence of $(\nu_R, \bar{\nu}_L)$ and boosts the importance of $0\nu\beta\beta$ decay.
- 2001-2006, Heidelberg-Moscow Coll. stated the observation of $0\nu\beta\beta$ decay in ^{76}Ge ($T_{1/2}^{0\nu} = 2.23^{+0.44}_{-0.31} \times 10^{25}$ yr)
- 2010-2013, the claim of Heidelberg-Moscow Coll. was overruled by the constraints from the cosmology observations and the latest data released by the EXO-200, KamLAND-Zen and GERDA collaborations.

Neutrinoless double beta decay: current status

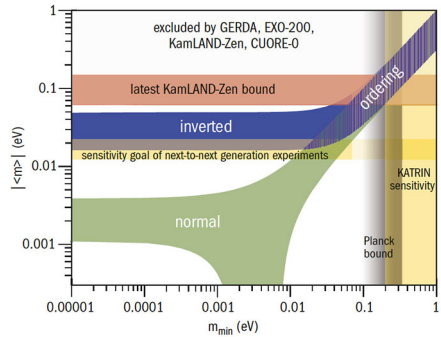
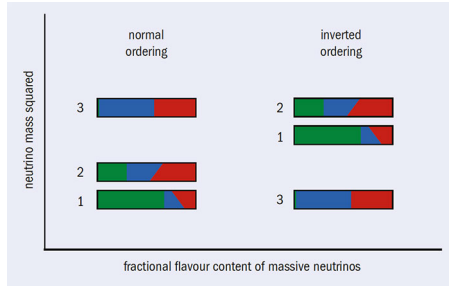


- Current experimental limits on the half-lives are at the level of
 $> 8.0 \times 10^{25}$ yr for ${}^{76}\text{Ge}$ and
 $> 1.07 \times 10^{26}$ yr for ${}^{136}\text{Xe}$

Isotope	$T_{1/2}^{0\nu} (\times 10^{25} \text{ yr})$	$\langle m_{\beta\beta} \rangle (\text{eV})$	Experiment
${}^{48}\text{Ca}$	$> 5.8 \times 10^{-3}$	$< 3.5 - 22$	ELEGANT-IV
${}^{76}\text{Ge}$	> 8.0	$< 0.12 - 0.26$	GERDA
	> 1.9	$< 0.24 - 0.52$	MAJORANA DEMONSTRATOR
${}^{82}\text{Se}$	$> 3.6 \times 10^{-2}$	$< 0.89 - 2.43$	NEMO-3
${}^{96}\text{Zr}$	$> 9.2 \times 10^{-4}$	$< 7.2 - 19.5$	NEMO-3
${}^{100}\text{Mo}$	$> 1.1 \times 10^{-1}$	$< 0.33 - 0.62$	NEMO-3
${}^{116}\text{Cd}$	$> 1.0 \times 10^{-2}$	$< 1.4 - 2.5$	NEMO-3
${}^{128}\text{Te}$	$> 1.1 \times 10^{-2}$	—	—
${}^{130}\text{Te}$	> 1.5	$< 0.11 - 0.52$	CUORE
${}^{136}\text{Xe}$	> 10.7	$< 0.061 - 0.165$	KamLAND-Zen
	> 1.8	$< 0.15 - 0.40$	EXO-200
${}^{150}\text{Nd}$	$> 2.0 \times 10^{-3}$	$< 1.6 - 5.3$	NEMO-3

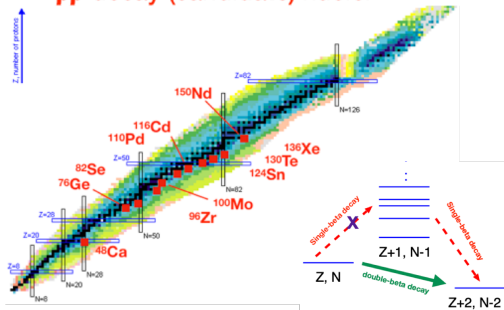
M. J. Dolinski et al. (2019)

Neutrinoless double beta decay: current status



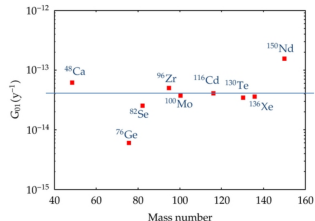
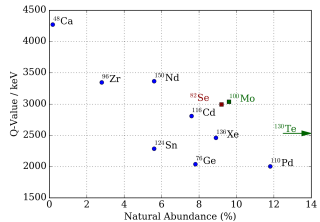
- The next-generation ton-scale experiments aiming at improvements in sensitivity by two orders of magnitude and will constrain the $\langle m_{\beta\beta} \rangle$ down to 10^{-2} eV in the near future.

$\beta\beta$ decay (candidate) nuclei



$$[T_{1/2}^{0\nu}]^{-1} = G_{0\nu} \left| \frac{\langle m_{\beta\beta} \rangle}{m_e} \right|^2 |M^{0\nu}|^2$$

where the phase-space factor $G_{0\nu}$ ($\sim 10^{-14} \text{ yr}^{-1}$) can be evaluated precisely Kotila ('12), Stoica ('13). The effective neutrino mass is related to the masses m_k and mixing matrix elements U_{ek} of neutrino species



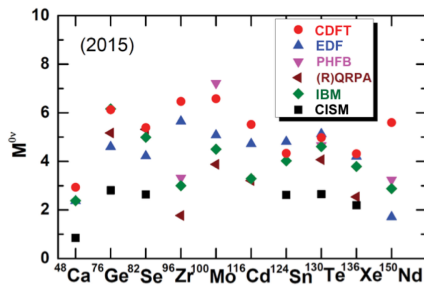
Nuclear matrix elements for neutrinoless double beta decay



The nuclear matrix elements for the $0\nu\beta\beta$ decay is determined by

$$M^{0\nu} = \langle \Psi_F | \hat{O}^{0\nu} | \Psi_I \rangle$$

- Transition operator (LNV processes, high-energy physics)
- Nuclear wave functions (many-body correlation, low-energy physics)



Note: only the calculations with $g_A(0)=1.25/1.26$ and considering the SRC effect with the UCOM [except for the IBM2 calculation with the coupled-cluster model (CCM)] and using the radius parameter $R = 1.2A^{1/3}$ fm are adopted for comparison.

Large model uncertainty:
Factors of 2-3.

CDFT: JMY, L.S. Song, K. Hagino, P. Ring, J. Meng, [PRC91, 024316 \(2015\)](#)

EDF(D1S): T. R. Rodriguez and G. Martinez-Pinedo, [PRL 105, 252503 \(2010\)](#)

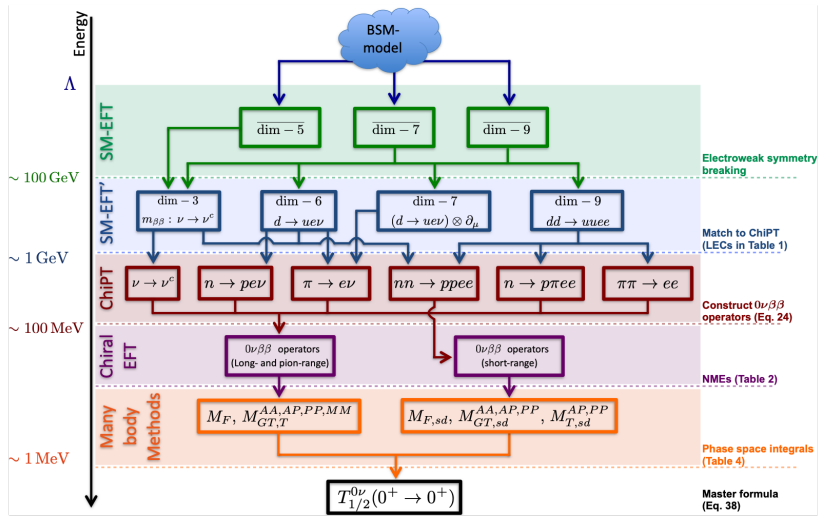
PHFB: P. K. Rath, R. Chandra, K. Chaturvedi, P. K. Raina, and J. G. Hirsch, [PRC 82, 064310 \(2010\); ibid. 88, 064322 \(2013\)](#).

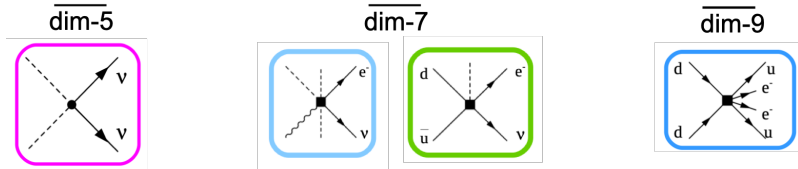
(R)QRPA : A. Faessler *et al.*, [J. Phys. G: Nucl. Part. Phys. 39, 124006 \(2012\)](#).

IBM: J. Barea and F. Iachello, [PRC79, 044301 \(2009\); J. Barea, J. Kotila, and F. Iachello, PRC87, 014315 \(2013\)](#)

CISM: J. Menendez *et al.*, [Nucl. Phys. A 818, 139 \(2009\)](#).

Transition operator for neutrinoless double beta decay





At the energy scale $\Lambda \gg v = (\sqrt{2}G_F)^{-1/2} = 2M_W/g \sim 246$ GeV:

- The dimension-5 operators ($\Delta L = 2$) induce a Majorana mass for neutrinos (Weinberg (1979))

$$\left(\frac{u_{\alpha\beta}}{\Lambda} \epsilon_{ij} \epsilon_{mn} H_j H_n \right) (L_i^{T\alpha} C L_m^\beta) + H.c. \quad (4)$$

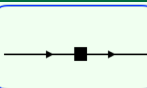
where $\alpha, \beta \in e, \mu, \tau, i, j, m, n$ are SU(2) indices. $u_{\alpha\beta}$ is a 3×3 matrix and

$L = (\nu_L, e_L)^T$ is the left-handed S(2) lepton doublet.

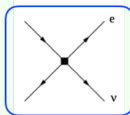
- The dimension-7 operators: $(v/\Lambda)^3$
- The dimension-9 operators: $(v/\Lambda)^5$

V. Cirigliano et al., JHEP (2018)

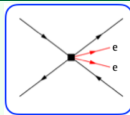
dimension-3 operators



dimension-6(7) operators



dimension-9 operators



- The heavy fields (W, Z, H , etc) are integrated out. The dimension-3 operators for the $0\nu\beta\beta$: (v/Λ)

$$\mathcal{L}_{\Delta e=0} = -\frac{1}{2}(m_\nu)_{ij}\nu_{L,i}^T C \nu_{L,j} + \dots, \quad m_\nu \sim \mathcal{O}(v^2/\Lambda)$$

- The dimension-6 (-7) operators: $(v/\Lambda)^3$

$$\mathcal{L}_{\Delta e=1} = \frac{2G_F}{\sqrt{2}} \left[C_{VL,ij}^{(6)} (\bar{u}_L \gamma^\mu d_L) (\bar{e}_R, i \gamma_\mu C \bar{\nu}_{L,j}^T) + \dots \right] + H.c.$$

- The $\Delta L = 2$ dimension-9 operators: $(v/\Lambda)^5, (v/\Lambda)^3$

$$\begin{aligned} \mathcal{L}_{\Delta e=2} &= \frac{1}{v^5} \sum_i \left[(C_{iR}^{(9)} \bar{e}_R C \bar{e}_R^T + C_{iL}^{(9)} \bar{e}_L C \bar{e}_L^T) O_i \right. \\ &\quad \left. + (C_i^{(9)} \bar{e}_L \gamma_m u \gamma_5 C \bar{e}^T) O_i^\mu \right], \end{aligned}$$

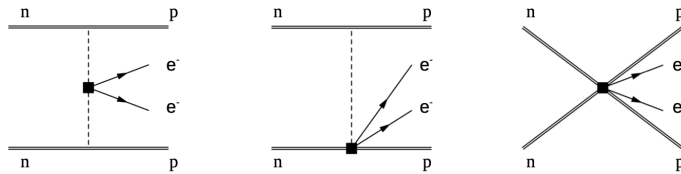
where O_i, O_i^μ are four-quark operators that are Lorentz scalars and vectors.

V. Cirigliano et al., JHEP (2018)

Neutrinoless double beta decay: in chiral perturbation theory

- Matching quark-level theory onto chiral perturbation theory, which describes interactions in low-energy in terms of baryons, mesons, photons and leptons.
- Write down all possible terms that have the same chiral symmetry properties under $SU(2)_L \times S(U2)_R$ as the quark-level operators and organize them as an expansion in terms of (p/Λ_χ)

dimension-9 operators V. Cirigliano et al., JHEP (2018)



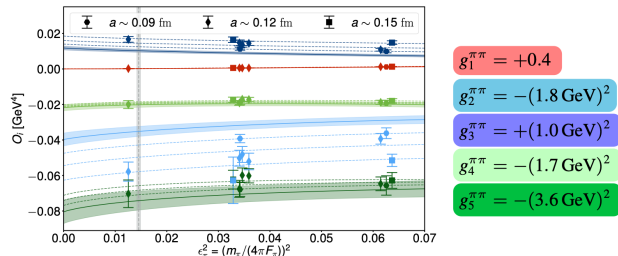
$$\begin{aligned} \mathcal{L} = & \left\{ \frac{F_0^2}{2} \left[\frac{5}{3} g_1^{\pi\pi} C_{1L}^{(9)} \partial_\mu \pi^- \partial^\mu \pi^- + \left(g_4^{\pi\pi} C_{4L}^{(9)} + g_5^{\pi\pi} C_{5L}^{(9)} - g_2^{\pi\pi} C_{2L}^{(9)} - g_3^{\pi\pi} C_{3L}^{(9)} \right) \pi^- \pi^- \right] \right. \\ & + \sqrt{2} g_A g_1^{\pi N} C_{1L}^{(9)} F_0 \bar{p} S \cdot (\partial \pi^-) n \\ & \left. + \left(g_1^{NN} C_{1L}^{(9)} + g_2^{NN} C_{2L}^{(9)} + g_3^{NN} C_{3L}^{(9)} + g_4^{NN} C_{4L}^{(9)} + g_5^{NN} C_{5L}^{(9)} \right) (\bar{p} n) (\bar{p} n) \right\} \frac{\bar{e}_L C \bar{e}_L^T}{v^5} + (L \leftrightarrow R) \end{aligned}$$

Neutrinoless double beta decay: in chiral perturbation theory



- Matching quark-level theory onto chiral perturbation theory, which describes interactions in low-energy in terms of baryons, mesons, photons and leptons.
- Write down all possible terms that have the same chiral symmetry properties under $SU(2)_L \times S(U2)_R$ as the quark-level operators and organize them as an expansion in terms of (p/Λ_χ)

dimension-9 operators V. Cirigliano et al., JHEP (2018)



A. Nicholson et al., Callat collaboration, '18

- $\pi\pi$ matrix elements well determined in LQCD

Neutrinoless double beta decay: low-energy nuclear many-body



- The nuclear Hamiltonian for calculating $0\nu\beta\beta$ decay:
V. Cirigliano et al., PRC (2018)

$$H_{\text{eff}} = H_{\text{strong}} + \sqrt{2} G_F V_{ud} j^\mu \mathcal{J}_\mu^\dagger + 2 G_F^2 V_{ud}^2 m_{\beta\beta} (\bar{e}_L C \bar{e}_L^T) \textcolor{red}{V}_\nu, \quad (5)$$

where the currents for leptons and nucleons (in NR form) are

$$j^\mu(x) = \bar{e}_L(x) \gamma^\mu \nu_L(x), \quad J_\mu = \sum_n^A (g_V \delta_{\mu 0} - g_A \delta_{\mu i} \sigma_i^{(n)}) \tau_+^{(n)} \quad (6)$$

- The $\Delta L = 2$ potential V_ν :

$$\textcolor{red}{V}_\nu = \sum_{a \neq b} \left[V_{\nu,0}^{(a,b)} + V_{\nu,2}^{(a,b)} + \dots \right] \quad (7)$$

where the LO neutrino potential by tree-level neutrino exchange plus the N²LO correction to the single-nucleon currents

$$V_{\nu,0}^{(a,b)} = \tau_+^{(a)} \tau_+^{(b)} \frac{1}{q^2} \left[h_F(q^2) - h_{GT}(q^2) \sigma^{(a)} \cdot \sigma^{(b)} - h_T(q^2) S^{(ab)} \right] \quad (8)$$

Neutrinoless double beta decay: low-energy nuclear many-body



- The $\Delta L = 2$ potential V_ν :

$$V_\nu = \sum_{a \neq b} \left[V_{\nu,0}^{(a,b)} + V_{\nu,2}^{(a,b)} + \dots \right] \quad (9)$$

where the $V_{\nu,2}^{(a,b)}$ is induced by one-loop diagrams [V. Cirigliano et al., \(2018\)](#)

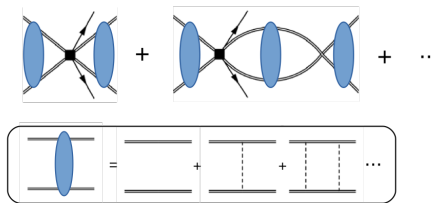
$$V_{\nu,2}^{(a,b)} = \tau_+^{(a)} \tau_+^{(b)} \left[V_{VV}^{(a,b)} + V_{AA}^{(a,b)} + \tilde{V}_{AA}^{(a,b)} \ln \frac{m_\pi^2}{\mu_{us}^2} + V_{CT}^{(ab)} \right] \quad (10)$$

where the contact term is ($F_\pi = 92.2$ MeV)

$$V_{CT}^{(ab)} = -\frac{2g_\nu^{NN}}{(4\pi F_\pi^2)^2} I^{(a)} \times I^{(b)}. \quad (11)$$

The unknown parameter g_ν^{NN} might be determined from lattice QCD calculation or EM isospin violation processes. [V. Cirigliano et al., \(2018\)](#)

Neutrinoless double beta decay: short-range operator

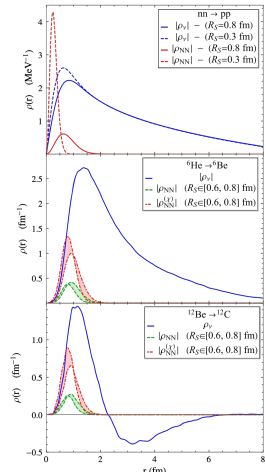


- Nuclear wave functions by variational Monte Carlo based on the AV18 two-nucleon and IL7 three-nucleon interactions
- Effect of the leading-order short-range operator (regulator dependent)

$$\delta M^{0\nu} = \int dr \rho_{NN}(r) \quad (12)$$

- The partial cancellation between the regions with $r \leq 2$ fm and $r \geq 2$ fm enhances the short-range contribution.

Extension to $0\nu\beta\beta$ candidate nuclei ...



V. Cirigliano et al., (2018)

Two-neutrino DBD



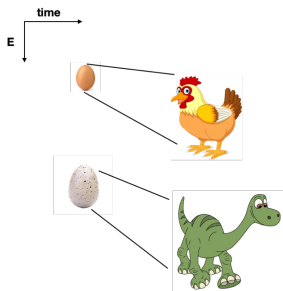
Nuclide	$T_{1/2}^{2\nu\beta\beta}$ \pm stat \pm sys [y]	rel. uncert. [%]	$G^{2\nu}$ $[10^{-21} \text{ y}^{-1}]$	$M^{2\nu}$ $[\text{MeV}^{-1}]$	rel. uncert. [%]	Experiment (year)
^{136}Xe	$2.165 \pm 0.016 \pm 0.059 \cdot 10^{21}$	± 2.83	1433	0.0218	± 1.4	EXO-200 (2014)
^{76}Ge	$1.84^{+0.09+0.11}_{-0.08-0.06} \cdot 10^{21}$	$+7.7$ -5.4	48.17	0.129	$+3.9$ -2.8	GERDA [39] (2013)
^{130}Te	$7.0 \pm 0.9 \pm 1.1 \cdot 10^{20}$	± 20.3	1529	0.0371	± 10.2	NEMO-3 [40] (2011)
^{116}Cd	$2.8 \pm 0.1 \pm 0.3 \cdot 10^{19}$	± 11.3	2764	0.138	± 5.7	NEMO-3 [41] (2010)
^{48}Ca	$4.4^{+0.5}_{-0.4} \pm 0.4 \cdot 10^{19}$	$+14.6$ -12.9	15550	0.0464	$+7.3$ -6.4	NEMO-3 [41] (2010)
^{96}Zr	$2.35 \pm 0.14 \pm 0.16 \cdot 10^{19}$	± 9.1	6816	0.0959	± 4.5	NEMO-3 [42] (2010)
^{150}Nd	$9.11^{+0.25}_{-0.22} \pm 0.63 \cdot 10^{18}$	$+7.4$ -7.2	36430	0.0666	$+3.7$ -2.7	NEMO-3 [43] (2009)
^{100}Mo	$7.11 \pm 0.02 \pm 0.54 \cdot 10^{18}$	± 7.6	3308	0.250	± 3.8	NEMO-3 [44] (2005)
^{82}Se	$9.6 \pm 0.3 \pm 1.0 \cdot 10^{19}$	± 10.9	1596	0.0980	± 5.4	NEMO-3 [44] (2005)

How to choose the reference state?

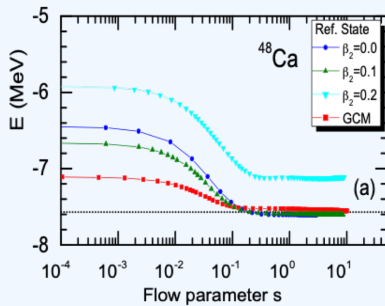
The choice of the reference state with density matrix elements living in a small model space provides an economic way to solve the IMSRG flow.

Can we choose the reference arbitrarily?

- You can choose **any reference state** you want, but if you choose the wrong one, you'll be sorry.

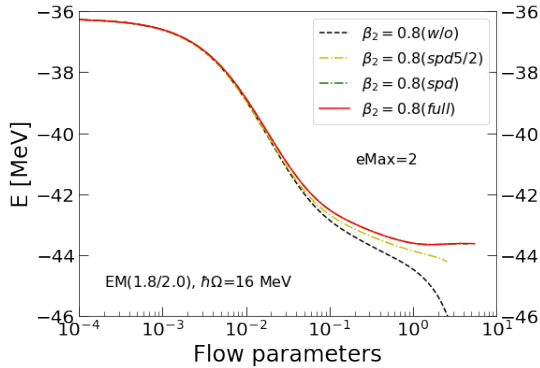


Calculation with KB3G interaction

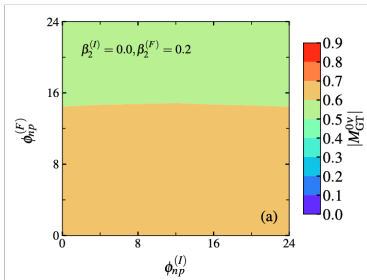


JMY, J. Engel, L. J. Wang, C.F. Jiao, H. Hergert (2018)

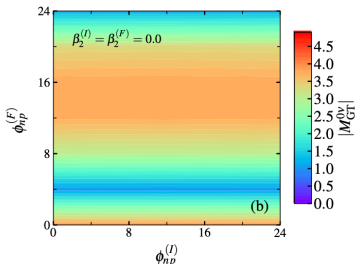
Impact of three-body irreducible density: ${}^8\text{Be}$



Application: $0\nu\beta\beta$ from ^{48}Ca to ^{48}Ti



(a)

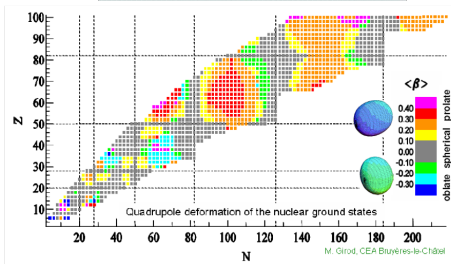
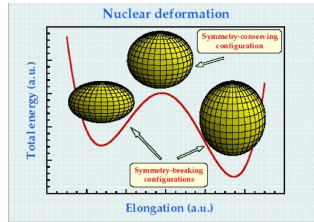


(b)

- The impact of ϕ_{np} in ^{48}Ca on $M^{0\nu}$ is negligible.

Strong collective correlations in open-shell nuclei

- Most **open-shell nuclei** gain additional energies through **deformations** in intrinsic frame.
- In mean-field (HFB) models, the **symmetry-breaking mechanism** provides an economic way to consider this effect.
- In shell models, the configurations of **many-particle many-hole excitations** are crucial to capture these effects.



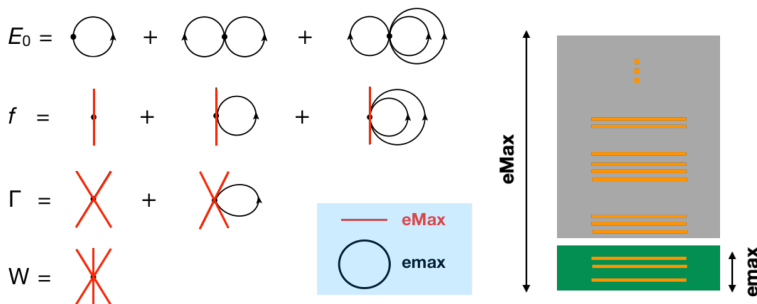
The method: density matrices in a small model space



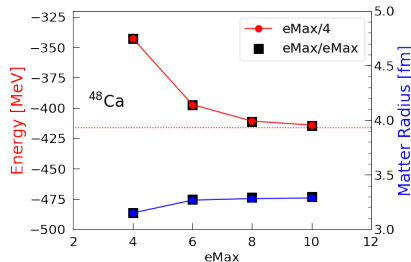
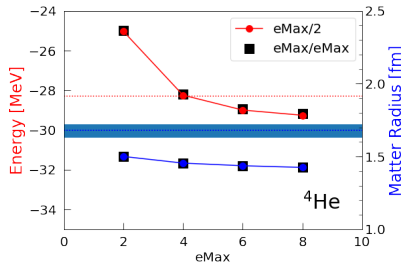
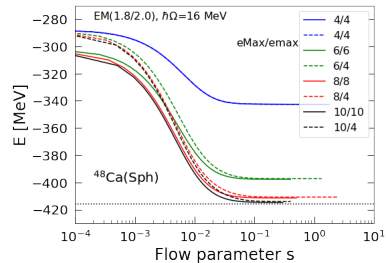
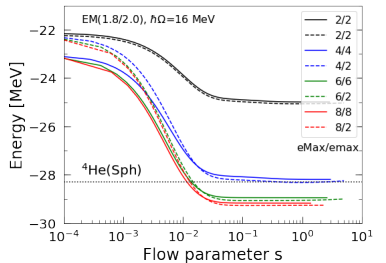
In no-core calculation, computation of many-body density matrices for a multi-reference state becomes difficult.

Prescription

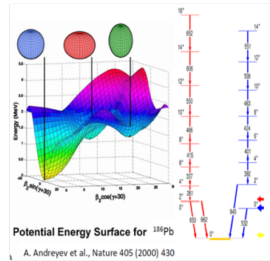
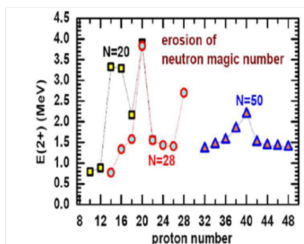
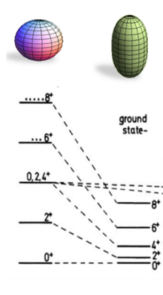
- Construct density matrix elements in a small model space (defined by e_{max})
- Normal-order the H and solve the IMSRG flow in a large model space (e_{Max})



The method: density matrices in a small model space



Collective correlations in nuclear low-lying states



- Nuclear low-lying states governed by the interplay of s.p. excitations and collective excitations
- For even-even nuclei, **strong collective correlations** (small shell gap) can be indicated from **low excitation energies** of first 2^+ state and **large $E\lambda$** transitions.
- Emergence of many interesting phenomena
clustering structure, shape transition, coexistence of different shapes, etc.